Estimation of the intrinsic heterogeneity of ionic glass-forming melts

V. Sh. Machavariani and A. Voronel
Raymond and Beverly Sackler School of Physics and Astronomy, Tel-Aviv University, Ramat-Aviv, 69978, Israel
(Received 7 July 1999)

The supercooled ionic melt is considered as a kind of binary composite material with an intrinsic heterogeneity (liquid medium and denser packed clusters) dependent on temperature. The conductivities of phases are extracted from the high (liquid) and low (glass) temperature experimental data. Effective conductivity of such a composite has been estimated using the checkerboardlike model with the presence of heterogeneity on different length scales. Using this model the volume fraction of the denser inclusions from experimental data on $Ca_2K_3(NO_3)_5$ and Zr-Ba-La-Al-Na-F compound glass formers has been estimated.

PACS number(s): 64.70.Pf, 72.80.Ng, 66.10.Ed

A lot of experimental data on ionic melts have been published [1–3] recently. These data are of special interest in the supercooled state of the melts. The supercooled melt has been considered by many recent theories [4] as a sort of dynamically heterogeneous medium. Whatever the reason for the emergence of this heterogeneity, the corresponding liquid on its nanometric scale can be presented as a composite material with inclusions of greater rigidity (and probably of a higher density) [5,6] which live much longer than a reorientation time of an individual molecule [6].

This paper is an attempt to use the experimental data on ionic melts in supercooled state for quantitative estimation of their intrinsic heterogeneity. The results of this estimation from independent conductivity and density experimental data on $Ca_2K_3(NO_3)_5$ (Refs. [1,2]) and ZBLAN20 ($0.53\,ZrF_4 - 0.20\,BaF_2 - 0.04\,LaF_3 - 0.03\,AlF_3 - 0.20\,NaF$, Ref. [3]) glass formers have been shown to be in a good agreement.

In 1970 Dykhne [7] has found that the effective conductivity σ_{eff} of infinite 2D checkerboard has the form

$$\sigma_{\text{eff}} = \sqrt{\sigma_w \sigma_b}, \tag{1}$$

where σ_w and σ_b are the conductivities of the white and black squares, respectively. The result of Eq. (1) is equally valid for triangular two-dimensional (2D) lattice and any random isotropic distribution of black and white spots of arbitrary shape until their surface concentrations are equal.

Let us consider the infinite 2D checker board whereby each ''black'' and ''white'' squares of this board are not uniform. Let the ''black'' squares be in their turn checker boards (not infinite) of ''green'' and ''blue'' squares (with conductivities σ_1 and σ_2, respectively); and let the ''white'' squares be checker boards (not infinite) of ''red'' and ''yellow'' squares (with conductivities σ_3 and σ_4, respectively). In this case $\sigma_b \approx \sqrt{\sigma_1 \sigma_2}$, $\sigma_w \approx \sqrt{\sigma_3 \sigma_4}$, and $\sigma_{\text{eff}} \approx \sqrt[4]{\sigma_1 \sigma_2 \sigma_3 \sigma_4}$.

This construction is illustrated in Fig. 1(a). Instead of the ''equal'' sign we have used ''approximately equal'' because of the finite (not infinite) size of ''blue-green'' and ''red-yellow'' checker boards. The larger the number of squares in these boards, the more accurate the equations are. Such a construction physically corresponds to the presence of different length scales: medium range order, short range order, etc.

Repeating this construction a number of times leads to the following expression:

$$\ln \sigma_{\text{eff}} \approx \sum_i n_i \ln \sigma_i, \tag{2}$$

where n_i is the concentration of the ith component. For Fig. 1 all n_i are equal to 1/4. But if some of the σ_i are equal to each other, different values for n_i follow. The analogous consideration is valid for triangular lattice and random distribution of the spots. For the case of arbitrary random distribution of domains, the Eq. (2) becomes approximate. But recent calculations of resistivity for composites with clusters of different shapes [8] have shown that the reasonable devia-

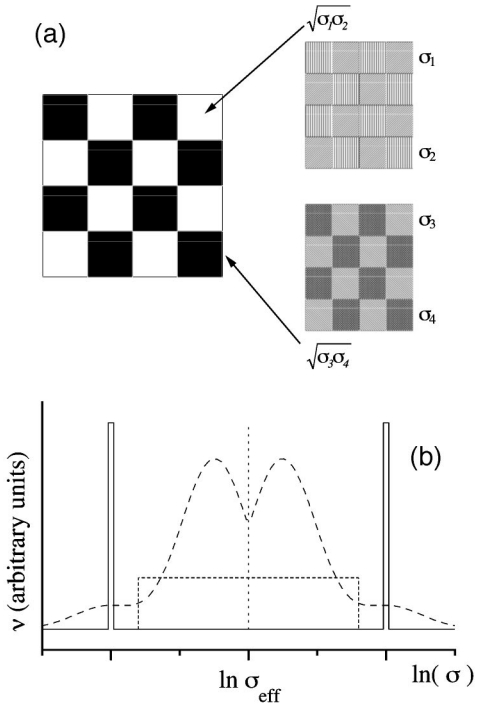

FIG. 1. (a) The schematic illustration of the model used. The white and black squares of the left checker board are not homogeneous. They in their turn are also checker boards (right part). (b) Schematic presentation of the probability density of the local conductivity for validity of Eqs. (2) and (3) in 2D case.

tions of clusters from the cubic form change the effective resistivity of the composite insignificantly (no more than 40%).

If the conductivity of the surface $\sigma=\sigma(x,y)$ depends smoothly on the local coordinates (x,y), then $\nu(\sigma)\Delta\sigma$ is the probability of the conductivity at the arbitrary point to be within the interval from σ to $\sigma+\Delta\sigma$. It has been shown by Dykhne [7] that the exact expression for the effective conductivity is going to be equal to

$$\ln\sigma_{\text{eff}}=\int \nu(\sigma)d(\ln\sigma) \tag{3}$$

under conditions that the effective conductivity of the infinite surface is isotropic and the probability density ν as a function of $\ln\sigma$ is symmetric. Figure 1(b) presents schematically some of the possible cases. Solid bars correspond to the case of two colored square, triangular or random array of spots.

The dashed curves correspond to the cases of some smooth conductivity distributions. Tortet *et al.* [9] have successfully used the rectangular distribution [see Fig. 1(b), dotted lines] of an active part of conductivity to describe the impedance data on composite (''brushite'') material.

In this paper we have performed a numerical calculation of 2D and 3D checker boards. The result of our computation for 2D cases (both square and triangular) have been compared to the exact 2D solution [7]. Our computational algorithm gives the conductivity σ_{calc} monotonically approaching from below ($\sigma_{\text{calc}}<\sigma_{\text{eff}}$) to the exact value (for $N\to\infty$).

The algorithm approximates the system of materially continuous squares (or triangles) by a square (or correspondingly, triangular) network of conducting wires. Each square (or triangle) is divided into M^2 equal cells. The center of each cell is connected to the centers of 4 (or 3) of the nearest neighboring cells by conducting wires. The resistance of the wire connecting the ith and jth cells is equal to $(\sigma_i+\sigma_j)/A\sigma_i\sigma_j$, where σ_i and σ_j are the conductivities of the ith and jth cells, respectively, M is the number of grid points in the edge of each square (or triangle), a coefficient $A=2$ for the square lattice and $A=2\sqrt{3}$ for the triangular one. Translational symmetry of the problem has been taken into account by choosing the periodical boundary condition for currents. The symmetry planes of the problem have been taken into account to reduce the computational time for solving the system of $N=2M^2$ linear algebraic equations.

This procedure can easily be generalized for the case of the 3D cubic checker board. The only difference now is that the number of cells in each cube is M^3; the number of the nearest neighbors is 6, the number of equations is $N=2M^3$ and the resistance of the wire between the centers of the ith and jth cells is $M[(\sigma_i+\sigma_j)/2\sigma_i\sigma_j]$. The maximal number of N used in our calculation is 13 718.

Figure 2(a) shows the deviations of the numerical result for the 2D square checker board from the exact solution $\Delta\sigma(N)=\sigma_{\text{eff}}-\sigma_{\text{calc}}(N)$ as functions of the number of linear equations N for the 3 different ratios $\gamma=\sigma_w/\sigma_b$. The linear form of these curves in log-log plot in 3 decades means that the deviation might be expressed by the formula $\Delta\sigma(N)=\alpha/N^{\beta}$.

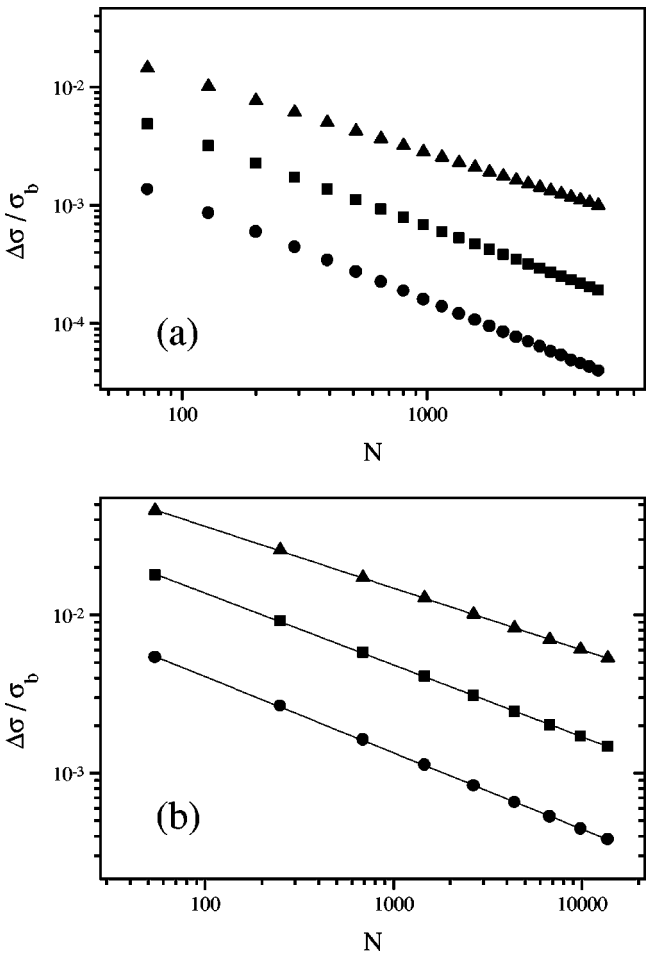

FIG. 2. (a) The deviation of the numerical result from the exact solution for 2D checker board as a function of the number of equations for different values of γ. (b) The deviation of the numerical result from the limiting value σ_∞ for 3D checker board as a function of the number of equations for different values of γ. (a) and (b) Triangles correspond to the case of $\gamma=0.3$, squares– $\gamma=0.5$, and circles– $\gamma=0.7$.

If one assumes the same kind of dependence to be valid for the 3D checker board, one can estimate σ_∞ from the equation

$$\sigma_\infty-\sigma_{\text{calc}}(N)=\alpha'/N^{\beta'}, \tag{4}$$

where σ_∞ is an extrapolated limit of the numerical solution for an infinite number of equations. In Fig. 2(b) it is evident that the reasonable choice of σ_∞ values allows to present the deviation $\sigma_\infty-\sigma_{\text{calc}}(N)$ this way in the whole range of our calculations (in 3 decades).

Figure 3(a) demonstrates these σ_∞ values (circles) for the 3D case in comparison with the exact solution for the 2D case (solid curve) as a function of $\gamma=\sigma_w/\sigma_b$. It is amazing to find out how close this 3D calculation is to the 2D case for the s not close to zero. Nevertheless it might be expected since a single layer of cubes behaves exactly as a 2D checker board. Thus, the difference between 2D and 3D appears as a result of layers' interconnection only. In the 3D case $\sigma_\infty \geqslant \sqrt{\sigma_w\sigma_b}$ is in agreement with the result of Ref. [10].

Figure 3(a) corresponds to the equation $\sigma_{\text{eff}}=f(\gamma)\sqrt{\sigma_w\sigma_b}$, where $f(\gamma)$ is a function which expresses the

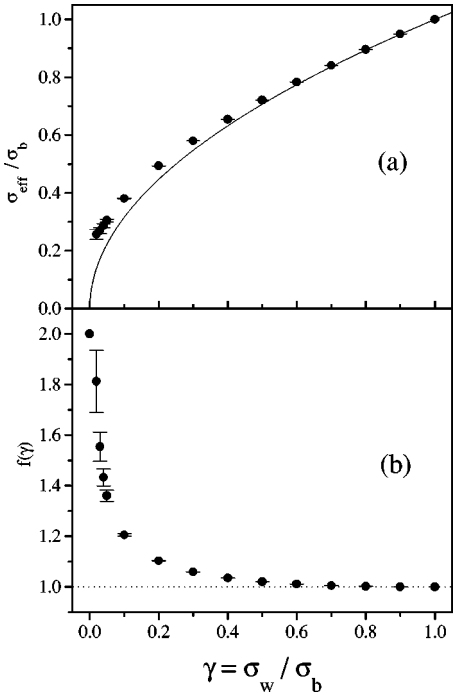

FIG. 3. (a) The effective conductivity for 3D (circles) and 2D (solid curve) checker boards as a function of $\gamma = \sigma_w / \sigma_b$. (b) The deviation function $f(\gamma)$.

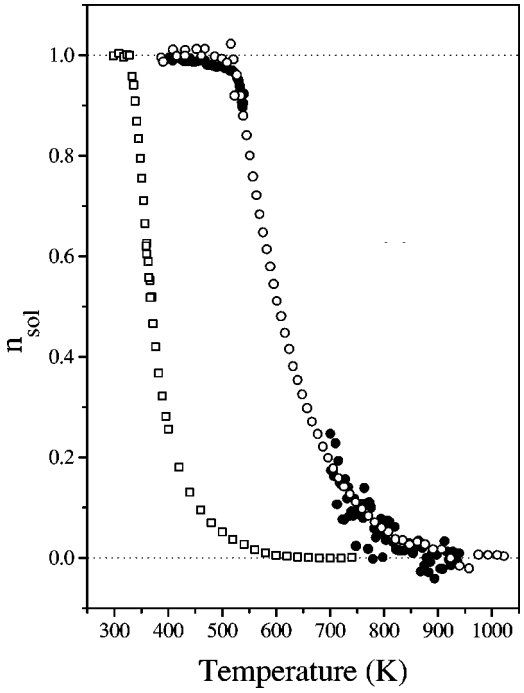

FIG. 4. The calculated volume fraction n_{sol} of the solid clusters in $Ca_2K_3(NO_3)_5$ (squares) and ZBLAN20 (circles) glass forming melts as a function of the temperature. Solid symbols are obtained from the density data, open symbols correspond to the resistivity data.

abovementioned deviation between 2D and 3D cases. Because of the symmetry relation $f(\gamma) = f(1/\gamma)$ one needs to calculate the function $f(\gamma)$ only for γ from 0 to 1. It was shown [11] that its asymptotic values are $f(0) = 2$, $f(1) = 1$. Figure 3(b) presents $f(\gamma)$ which is obtained from our calculation.

We have used the above consideration to describe the conductivity of ionic glass formers in their supercooled state. For this case σ_{eff} might change up to 10^{14} times. Thus, the whole range of the variation of the function $f(\gamma)$ is not important. That is why one can use the Eq. (2) as the first approximation for the 3D case.

Now let us apply this approach to the experimental data on CKN [1,2] and ZBLAN20 [3]. Actually there is, probably, a whole spectrum of local conductivities in glassifying liquid. But let us consider for the sake of simplicity a glass former in its nanometric scale being a mixture of two components only. The first component is the ''liquidlike'' one with the conductivity σ_{liq} and the volume fraction n_{liq}. The conductivity for this component may be extrapolated from a high temperature region (Arrhenius [1,12] behavior) of the corresponding glass former $\sigma_{liq} = (A_{liq}/T)\exp(E_{liq}/T)$, where T is a temperature, E_{liq} is an activation energy of the liquid state (in K), A_{liq} is a material dependent constant. The second component consists of the ''solidlike'' clusters of random form and size with conductivity σ_{sol} and volume fraction $n_{sol} = 1 - n_{liq}$, where σ_{sol} can be extracted from the glass behavior below T_g in an analogous way: $\sigma_{sol} = (A_{sol}/T)\exp(E_{sol}/T)$. Here E_{sol} is the activation energy in the glassy state (usually 2–4 times higher than E_{liq}).

Therefore, one can extract from the experimental data the temperature dependence of the volume fraction of the solid component n_{sol} using the equation (2) and the extrapolated values of σ_{sol} and σ_{liq}:

$$n_{sol}(T) \approx \frac{\ln \sigma_{liq}(T) - \ln \sigma_{eff}(T)}{\ln \sigma_{liq}(T) - \ln \sigma_{sol}(T)}. \tag{5}$$

Another way to estimate the n_{sol} is to use the density data. In both liquid and glassy states the density is roughly a linear function of the temperature. If one assumes the density of both ''solidlike'' inclusions d_{sol} and ''liquidlike'' medium d_{liq} to be equal to the extrapolated values from the low and high temperature region respectively, one can estimate the n_{sol} in the following way:

$$n_{sol}(T) = \frac{d(T) - d_{liq}(T)}{d_{sol}(T) - d_{liq}(T)}, \tag{6}$$

where $d(T)$ is the experimentally measured density of the glass former.

The result for $n_{sol}(T)$ is presented in Fig. 4 as a function of temperature. We have used our data [1] and data by Angell [2] on $Ca_2K_3(NO_3)_5$ conductivity and the data by Hasz [3] on ZBLAN20's conductivity and density. Unfortunately, while the conductivity which varies in orders can be measured with precision, the density which varies in 20% only is measured relatively less accurately. The agreement of n_{sol} obtained from conductivity and density data confirms the physical meaningfulness of Eqs. (5) and (6). Let us note the different character of the two curves corresponding to two different glass forming abilities of the CKN and ZBLAN20.

The dc conductivity of the glassy state at $T < T_g$ is extremely small. Thus the ''solidlike'' inclusion in liquid medium behaves as a capacitor. At high frequencies this capacitance might become dominant in ac conductivity measurement $\sigma(\omega)$: $\sigma(\omega) \propto (\omega)^{n_{sol}}$. This effect corresponds

to the well known ''universal conductivity response'' (Ref. [13]) which was found to be universal for the strongly disordered systems (glasses, etc.): $\sigma(\omega)=\sigma_0[1+(\omega\tau)^s]$. Here ω is a frequency, τ is an effective relaxation time, s is a characteristic exponent, $0<s<1$. For high frequency [13] or/and low temperature s is approaching to 1. For the low frequency [13] or/and high temperature s is always less than 1.

Thus our ''compositelike'' picture is consistent with the ''universal conductivity response'' and gives the exponent s the sense of the volume fraction of the solid component (especially for low temperature limit). The lower the temperature, the closer the index s is to 1 because the volume fraction of the solid component increases. The higher the frequency, the closer the index s is to 1 because the imaginary part of the σ_{sol} becomes dominant. For high temperature and/or low frequency, our model predicts that s vanishes. However, for high temperature limit, the small clusters with intermediate conductivity probably become important. That is why for the description of the ac conductivity behavior at high temperature, one needs to take into account the possible distribution of local conductivities.

This work was supported by The Aaron Gutwirth Foundation, Allied Investments Ltd. (Israel). The authors are grateful to Dr. W. C. Hasz for his kind readiness to provide us with the experimental data on ZBLAN20 melt and to Dr. L. Fel for the useful discussion.

[1] A. Voronel, E. Veliyulin, V.Sh. Machavariani, A. Kisliuk, and D. Quitmann, Phys. Rev. Lett. **80**, 2630 (1998).

[2] C.A. Angell, J. Phys. Chem. **68**, 1917 (1964); R. Weiler, S. Blaser, and P.B. Macedo, *ibid.* **73**, 4147 (1969); H. Tweer, N. Laberge, and P.B. Macedo, J. Am. Ceram. Soc. **54**, 121 (1971).

[3] W.C. Hasz, J.H. Whang, and C.T. Moynihan, J. Non-Cryst. Solids **161**, 127 (1993).

[4] S.S. Ghosh and C. Dasgupta, Phys. Rev. Lett. **77**, 1310 (1996); W. Kob, C. Donati, S.J. Plimpton, P.H. Poole, and S.C. Glotzer, *ibid.* **79**, 2827 (1997); F. Stillinger, J. Chem. Phys. **89**, 6461 (1988); F. Stillinger and J. Hodgdon, Phys. Rev. E **50**, 2064 (1994); T. Kirkpatrick, D. Thirumalai, and P. Wolynes, Phys. Rev. A **40**, 1045 (1989); R. Chamberlin and D. Kingsbury, J. Non-Cryst. Solids **172-174**, 318 (1994); J. Bendler and M. Schlesinger, J. Phys. Chem **96**, 3970 (1992); S. Kivelson, X. Zhao, D. Kivelson, T. Fisher, and C. Knobler, J. Chem. Phys. **101**, 2391 (1994).

[5] B. Gerharz, G. Meier, and E. Fisher, J. Chem. Phys. **92**, 7110 (1990); E. Fisher, E. Donth, and W. Steffen, Phys. Rev. Lett. **68**, 2344 (1992); G. Patterson and J. Stevens, J. Non-Cryst. Solids **172-174**, 311 (1994); W. Steffen, A. Patkowsky, G. Meyer, and E.W. Fisher, J. Chem. Phys. **96**, 4171 (1992).

[6] M. Cicerone and M. Ediger, J. Phys. Chem. **97**, 10 489 (1993); M. Cicerone, F. Blackburn, and M. Ediger, J. Chem. Phys. **102**, 471 (1995); K. Earl, J. Moscicki, A. Polimeno, and J. Freed, *ibid.* **106**, 9996 (1997); S. Sen and J.F. Stebbins, Phys. Rev. B **58**, 8379 (1998).

[7] A.M. Dykhne, Sov. Phys. JETP **32**, 63 (1970).

[8] J.F. Douglas and E.J. Garboczi, *Advances in Chemical Physics*, edited by I. Prigogine and S.A. Rice (Wiley, New York, 1995), Vol. XCI, p. 85.

[9] L. Tortet, J.R. Gavarri, J. Musso, G. Nihoul, G.P. Clerc, A.N. Lagarkov, and A.K. Sarychev, Phys. Rev. B **58**, 5390 (1998).

[10] K. Schulgasser, J. Math. Phys. **17**, 376 (1976).

[11] M. Söderberg and G. Grimvall, J. Phys. C **16**, 1085 (1983).

[12] E. Veliyulin, A. Voronel, and H.A. Oye, J. Phys.: Condens. Matter **7**, 4821 (1995); A. Voronel, E. Veliyulin, T. Grande, and H.A. Oye, *ibid.* **9**, L247 (1997).

[13] A.K. Jonscher, *Dielectric Relaxation in Solids* (Chelsea Dielectrics, London, 1983); A.V. Vaysleyb, Phys. Rev. B **58**, 8407 (1998).